

An Application of Geospatial Based MCDM Technique to Identify Landslide Susceptibility Zones in the Ragnu Khola River Basin of Darjeeling Himalayan Region, India

SATYAJIT DAS (✉ dassatyajit458@gmail.com)

University of North Bengal <https://orcid.org/0000-0002-3392-7932>

DIPESH ROY

University of North Bengal

RAJIB MITRA

University of North Bengal

Research

Keywords: Landslide susceptibility zones (LSZ), River morphometry, MCDM technique, ROC-AUC

Posted Date: December 23rd, 2021

DOI: <https://doi.org/10.21203/rs.3.rs-1147143/v1>

License: © ⓘ This work is licensed under a Creative Commons Attribution 4.0 International License.

[Read Full License](#)

An application of geospatial based MCDM technique to identify landslide susceptibility zones in the Ragnu Khola River Basin of Darjeeling Himalayan region, India

Authors Details

Satyajit Das^{1*} (Corresponding Author)

Research Scholar, Department of Geography and Applied Geography, University of North Bengal, Siliguri, West Bengal, India, Email: dassatyajit458@gmail.com, ORCID: 0000-0002-3392-7932.

Dipesh Roy¹

Research Scholar, Department of Geography and Applied Geography, University of North Bengal, Siliguri, West Bengal, India, Email: dipeshroy47@gmail.com, ORCID: 0000-0001-7686-5236.

Rajib Mitra¹

Research Scholar, Department of Geography and Applied Geography, University of North Bengal, Siliguri, West Bengal, India, Email: rajibmitrageo@gmail.com, ORCID: 0000-0002-3018-8935.

Abstract

Several natural disasters are taking place on the earth, and landslide is one of them. Darjeeling Himalaya is one of the world's young fold mountainous area, often suffering from landslide hazards. Hence, the study identifies the landslide susceptibility zone in the Ragnu Khola river basin of the Darjeeling Himalayan region by applying the geospatial-based MCDM technique. This research's major goal is to identify whether this GIS-based multi-criteria decision-making (MCDM) technique is validated or not for landslide susceptibility zones (LSZ); if validated, then how much manifest for describing the LSZ in the study area. MCDM evaluation applies to determining weight value to integrate different thematic layers of river morphometry like Drainage Diversity (DD) parameters and Relief Diversity (RD) parameters. Both DD and RD have significant impacts on landslide intensity. Hence, both layers are combined using the analytical hierarchy process (AHP) of the MCDM technique for the final LSZ. The final result has been validated by ROC analysis using landslide occurring point data obtained from the

Geological Survey of India (GSI). The outcome of the study shows that 1.45% and 17.83% areas of the region fall in 'very high' and 'high' LSZ, which belongs to near Mull Gaon, Sanchal forest, and Alubri basti. Most of the area (47.70%) is observed in 'moderate' LSZ. Only 1.32% and 31.7% are kept in 'very low' and 'low' LSZ, respectively, through the study area. The description capability of the technique for LSZ is significant as the area under the curve (AUC) is 72.10%. The validation of the study using the frequency density of the landslides (FDL) also indicates the 'very high' LSZ is associated with the maximum (2.19/km²) FDL. The work will be needful to develop the overall socio-economic condition of such kind of tectonically sensitive region by proper effective planning.

Keywords: Landslide susceptibility zones (LSZ); River morphometry; MCDM technique; ROC-AUC.

1. Introduction

A natural hazard is an extreme occurrence and harms humans or other things that we care about (White 1974). In mountainous regions, many natural hazards can happen in the form of landslides, avalanches, debris flows, and flash floods. Among them, landslides are the most common (Pourghasemi et al. 2012b). The saturation of soil and erosion of rock by water increased due to high rainfall, reduced plant cover, and rapid urban growth in the hilly areas. As a result, landslides occur on high gradient slopes in mountain areas (Chamling 2013; Bhattacharya 2013; Nad 2015). The occurrences of landslides are directly caused risks to human beings and losses in private and public assets (Petley 2012; Pourghasemi et al. 2012b). However, a study from 1964 to 1999 revealed that there is a positive increase in the number of landslide happening events around the world (Nadim and Kjekstad 2009). From 1990 to 2005, it accounted for 4.89% of all-natural disasters globally (www.em-dat.net). Landslide susceptibility zones (LSZ) must be identified before landslide mitigation measures may be implemented (Varnes 1984).

Landslides play the most widespread disaster in the Darjeeling Himalayan region. It is one of the world's young fold mountainous region. Climatic variability, tectonic disturbances, geological properties, and increased anthropogenic activity such as road, building, and resort construction have integratedly caused landslides in various regions of the Darjeeling Himalaya (Basu and Pal 2018). According to the expert opinion, several previous studies on landslide susceptibility mapping (LSM) were done based on manual interpretations of various thematic layers (Sarkar et al. 1995; Viridi et al. 1997). Researchers have used quantitative approaches in

contemporary periods, viz. artificial neural networks (Lucchese et al. 2021; Jacinth Jennifer and Saravanan 2021), logistic regression analysis (Gu et al. 2021; Crawford et al. 2021; Sujatha and Sridhar 2021), fuzzy logic (Bahrami et al. 2021; Manaouch et al. 2021; Nanehkaran et al. 2021), multivariate regression analysis (Arabameri et al. 2019; Chu et al. 2019; Pham et al. 2021), bivariate regression analysis (Zhou et al. 2021) to delineate LSZ. Machine learning approaches are now widely used to predict natural disasters such as floods, wildfires, earthquakes, and droughtiness, among others (Hong et al. 2018; Ahmadlou et al. 2019). The algorithms of the machine learning approaches are used for landslides hazard zonation, and also with the use of artificial neural networks (ANN), best-first decision tree (BFDT), logistic model tree (LMT) model (Shirzadi et al. 2017; Dou et al. 2018). Now, the importance of preparing the thematic layers of those factors that account for the zonation of potential landslide hazard areas is given in this study by using a multiple-criteria decision-making (MCDM) approach of various thematic layers from remotely sensed data (Saha et al. 2002, Sarkar and Kanungo 2004). Morphology is the measurement and quantitative investigation of the earth's surface and landforms (Clarke 1996; Agarwal 1998; Reddy et al. 2004). To understand the hydro-geological properties, morphometric analysis is very much essential. It also expresses the prevailing climatic, topographic, geological, and geomorphological conditions of the concerned area (Horton 1945; Strahler 1952; Hurtrez et al. 1999; Basu and Pal 2018).

The study has been conducted using morphometric variables to demonstrate the LSM of the Ragnu Khola River Basin in the Darjeeling Himalayan region. To achieve the goal, a large number of morphometric variables were taken into account. The two broad aspects of morphometric analysis used to identify LSZ, viz. drainage diversity (DD) and relief diversity (RD) (Pal and Saha 2017; Basu and Pal 2018; Basu and Pal 2019). In the present study, the authors have used the analytical hierarchy process (AHP) for the weight generation of different landslide susceptibility indicators. The AHP is a widely used strong MCDM technique for weighting the indicators (Navarro et al. 2019; Kaur et al. 2020; Zarei et al. 2021), postulated by Saaty (Saaty 2004; Saaty 2008). An attempt to check the final output map is also made during the accuracy assessment. The outcome of the work will aid government agencies, policymakers, and planners in reducing landslide-related damages and proper planning for land use in the areas with 'very high' landslides susceptibility of the Ragnu Khola River Basin.

2. Materials and methods

2.1. Study area

The Ragnu Khola River basin, considered the study area, is located in the Darjeeling district of West Bengal in India (Fig. 1). The latitudinal extension of this river basin is from 27° 00' 19''N to 27° 06' 30''N, the longitudinal extension is from 88° 16' 03''E to 88° 21' 21''E, and the basin area is about 64.79 km². The river Ragnu Khola is also known as the Rongdong River. It is a very small river basin originating from the eastern down part of the Darjeeling town. The drainage pattern of this river basin is the dendritic type which means that the river basin has structural control. The Ragnu Khola River finally meets with the Bari Rangit River, which is the major tributary of the Tista River. This river flows into the north-eastern direction based on the natural slope of the region. The basin elevation ranges from 230 to 2478 m, and most of the area is rocky type. The climatic condition of this river basin is monsoon type. Most of the rainfall happened during the monsoon period. The average annual rainfall of the region is approximately 3094.40 mm. In summer, the maximum temperature is about 26°C, while the minimum temperature is about 19°C. But in the winter season, it remains very low such as the maximum temperature is about 6°C and the minimum temperature is -2°C. Most of the landslides occur during the rainy season when heavy rainfall occurs in a short period.

[Fig. 1 Location map of the Ragnu Khola River Basin in the Darjeeling Himalaya]

2.2. Data acquisition and methods for LSM

For extracting the stream network of the Ragnu Khola River Basin, a toposheet has been collected from the Survey of India (SOI). The topographical map has the G45E8 number on 1:50000 scale. The map was georeferenced using ArcGIS software, and all stream networks of the study area were digitized. Along with this, the researchers also used STRM DEM (30 m) to delineate the basin with the help of the ArcGIS 'hydrology' tool. The necessary data and maps are also collected from the different government websites. The acquired datasets are mentioned in Table 1, and the methodological framework of the work is shown in Fig. 2. The essential part of delineating LSM is the selection of appropriate landslide conditioning indicators. Hence, the present study was considered based on the frequent landslide occurring factors used in several studies (Arabameri et al. 2017; Saleem et al. 2019; Liu et al. 2021). Here, 16 indicators are taken as landslide conditioning indicators, categorized into two broad groups: relief diversity (RD) and drainage diversity (DD). A detailed description of the RD and DD indicators are given below:

[Table 1 Data used and their sources to identify LSZ in the Ragnu Khola River Basin]

[Fig. 2 Methodological framework of the present study]

2.2.1. Relief diversity (RD) indicators

The basin elevation (Be) is vital in landslide conditioning indicators as its gravitational potential energy (Chen et al. 2019). Variation in elevation of any region affects the geomorphological features, nature of the vegetation, and degree of erosion. Thus, changes in elevation influence the landslide susceptibility (Chen et al. 2017). The relief map of the region is depicted in Fig. 3 (a). The slope (Sl) is considered the most significant indicator for mapping landslide susceptibility. It can be used to know the steepness of the topography (Chen et al. 2019), and it has a direct influence on occurrences of landslides. The 'Sl' map has been prepared from SRTM DEM (30 m resolution). The basin exhibits a variety in 'Sl', ranging from 0.33^0 to 59.42^0 , as displayed in Fig. 3 (b). As a topographic indicator, the aspect (As) affected the landslides, which are triggered due to rainfall (Beullens et al. 2014; Gorokhovich and Vustianiuk 2021). It is referred to as the direction of the slope of any region. It is interrelated with the microclimatic parameters and azimuth of the flow (Erener and Duzgun 2010; Mondal and Mandal 2019). It also affects the variation in temperature, relative humidity, and vegetation coverage of a slope (Bennie et al. 2006). The 'As' map of the study area is depicted in Fig. 3 (c). The landslide susceptibility mapping is interrelated with the lithological properties of that area (Pourghasemi et al. 2012a; Mandal and Maiti 2014). The rock strength and permeability of the land surface vary as per the lithological formations (Ayalew and Yamagishi 2005; Wang et al. 2020). The lithological data has been obtained from the Geological Survey of India (GSI). It manifested that three formations are present in the basin, i.e., Gorubathan, Kanchenjunga Gneiss, and Chungthang, as displayed in Fig. 3 (d). Most of the part of the basin is covered with the Kanchenjunga Gneiss formation. Ruggedness index (Ri) is used to understand the instability and structural complexity of the topography (Strahler 1956; Schumm 1956). The basin demonstrates the range of 'Ri' is from 0 to 3.12 (Fig. 3 e). It was computed using Eq. 2, where Ri stands for relative relief, Dd stands for drainage density, and K stands for constant (Patton and Baker 1976).

$$Ri = \frac{Rr \times Dd}{K}. \quad (2)$$

The presence of lineaments of any area directly influences landslide susceptibility (Keefer and Larsen 2007; Kaur et al. 2018). Hence, it has been taken as an essential landslide conditioning indicator. It represents the geomorphologic signatures like topographic breaks, shear zones, tectonic structures, and discontinuities (Sarkar and Kanungo 2004; Ayalew and

Yamagishi 2005). The lineament density (Ld) map of the basin is represented using the 'line density' tool in ArcGIS. The 'Ld' value ranges from 0 to 1.83 km/km² (Fig. 3 f). The Higher 'Ld' region has a high probability of frequent landslides (Erener and Duzgun 2010). Soil is an essential indicator for mapping landslides susceptibility because shallow depth soils are mostly affected during landslides (Sharma et al. 2012). In the study area, two soil classes are identified (Fig. 3 g) from the soil map of the NBSS and LUP. The classes are 'W002' (coarse loamy) and 'W004' (loamy-skeletal). Both soils are moderately shallow in-depth, and well-drained. 'W002' soil is associated with strong rockiness and severe erosion, while 'W004' soil has moderate rockiness and moderate erosion. Relative relief (Rr) is the difference in the highest and lowest altitude of a unit area. It is also known as 'amplitude of relief' or 'local relief' (Iqbal et al. 2021). It helps to analyze the morphological properties of the topography (Gayen et al. 2013; Basu and Pal 2019). The 'Rr' map of the study area is prepared using Eq. 1 by applying the grid method and the 'IDW' tool in ArcGIS. The basin represents the 'Rr' value varies from 140 to 895 m (Fig. 3 h). The formula of 'Rr' is as follows (Smith 1935):

$$Rr = H - h, \quad (1)$$

where, H is the highest altitude, and h is the lowest altitude of a unit area. The high 'Rr' zone is associated with landslide susceptible zones (Das and Lepcha 2019). Dissection index (Di) is one of the landslide conditioning parameters and has been considered by several researchers (Altin and Gokkaya 2018; Basu and Pal 2019; Das and Lepcha 2019). 'Di' is known as the ratio between the relative relief and absolute altitude (Nir 1957). It shows the stage of the landscape development and dissection of the river basin (Altin and Gokkaya 2018; Basu and Pal 2019). The study area reflects the 'Di' value varies from 0.05 to 0.58 (Fig. 3 i). The regions with high and very high 'Di' values are related to the steep sloping lands and high landslide susceptible zone.

[Fig. 3 Raster maps of different relief diversity parameters (a) Basin relief, (b) Slope, (c) Slope aspect, (d) Lithological formation, (e) Ruggedness index, (f) Lineament density, (g) Soil type, (h) Relative relief, and (i) Dissection index of the Ragnu Khola River Basin in the Darjeeling Himalaya]

2.2.2. Drainage diversity (DD) indicators

Drainage density (Dd) is used in the study as the drainage diversity (DD) parameter. 'Dd' is one of the prominent landslides conditioning indicators (Sahana and Sajjad 2017). It can be defined as follows (Strahler 1964):

$$Dd = \frac{L\mu}{A}, \quad (3)$$

where, $L\mu$ denotes the total length of the river, and A denotes the area drained. The higher 'Dd' areas are mainly associated with the regions with slope failure; hence, it caused landslides phenomena in the hilly watershed (Hasegawa et al. 2014). The value of 'Dd' in the study area ranges from 1.84 to 7.15 km/km² (Fig. 4 a). The factor stream frequency (Fs) has a direct relationship with the landslides. In this region, 'Fs' varies from 3 to 24 streams/km², as illustrated in Fig. 4 (b). The higher 'Fs' implies higher chances of landslides, and vice versa. For the present study, 'Fs' is computed using Eq. 4, as follows:

$$Fs = \frac{N\mu}{A}, \quad (4)$$

where $N\mu$ represents the total number of rivers, and A represents the area (Horton 1945). Drainage intensity (DI) is expressed as the ratio between stream frequency and drainage density (Faniran 1968). It represents the runoff characteristics of any region (Basu and Pal, 2019). Here, 'DI' ranges from 0.64 to 5.85, as depicted in Fig. 4 (c). Higher 'DI' areas are characterized with maximum possibilities of landslides hazard, while lower 'DI' areas are represented with less chances (Das and Lepcha 2019). Drainage texture (Dt) is associated with the rock, relief, soil, climate, and vegetation characteristics of any region (Kale and Gupta 2001). 'Dt' can be expressed as follows (Horton 1945):

$$Dt = \frac{N\mu}{P} \quad (5)$$

where, $N\mu$ is depicted as the number of streams, and P is depicted as the perimeter of the basin. The study area has 'Dt' value from 0 to 6 streams/km (Fig. 4 d). The stream junction frequency (Jf) is another crucial morphometric parameter of a river basin that influences landslides phenomena. 'Jf' is defined as the presence of stream junction points in each grid (Das and Lepcha 2019). It indicates the area with an instable slope; hence high 'Jf' value is caused landslides. The 'Jf' of the region ranges from 0 to 12.99. Infiltration number (In) as a morphometric parameter illustrated the runoff intensity and infiltration capacity of the region (Strahler 1964). The higher 'In' implies high runoff and low infiltration, and vice versa. The higher rate of infiltration accelerated the movement of landslides (Basu and Pal 2019). The 'In' is calculated for the present study area using the following equation (Zavoiance 1985):

$$In = Dd \times Fs \quad (6)$$

where, Dd represents the drainage density, and $F5$ represents the stream frequency. In the study area, 'In' is varies from 7.59 to 121.04 (Fig. 4 f). Length of overland flow (Lo) is used as an important morphometric parameter. In terms of hydrologic and physiographic growth, 'Lo' impacts the drainage basin (Horton 1932). Luo et al. (2015) investigated the influence of 'Lo' on shallow landslides caused by rainfall. The 'Lo' is calculated using the following equation (Horton 1945):

$$Lo = 1/2 \times Dd, \quad (7)$$

where, Dd is the drainage density. The study area exhibits the 'Lo' value ranges from 0.92 to 3.57 km, as depicted in Fig. 4 (g).

[Fig. 4 Raster maps of different drainage diversity parameters (a) Drainage density, (b) Stream frequency, (c) Drainage intensity, (d) Drainage texture, (e) Junction frequency, (f) Infiltration number, and (g) Length of overland flow of the Ragnu Khola River Basin in the Darjeeling Himalaya]

2.2.3. Weight value calculation by AHP

The work primarily focuses on preparing the DD and RD thematic layers. Hence, drainage density (Dd), drainage texture (Dt), drainage intensity (DI), infiltration number (In), stream frequency (Fs), length of overland flow (Lo), and junction frequency (Jf) factors were analyzed and combined to create the DD layer. On the other hand, the relief diversity (RD) layer was prepared by the integration of basin elevation (Be), soil type (St), dissection index (Di), ruggedness index (Ri), relative relief (Rr), slope (Sl), aspect (As), lithology (Lg), and lineament density (Ld) parameters (Pal and Saha 2017; Basu and Pal 2018; Basu and Pal 2019). Finally, LSM has been created using AHP techniques by integrating the RD and DD thematic layers with 50% weightage value for both in ArcGIS software. The AHP is a one-level scoring process that examines indicators using a pair-wise comparison matrix table (Saaty 1990). A nine-point scale (Table 2) is used to rate each criterion's relative preferences on each basis (Malczewski 2006). The scale was utilized to give a verbal expression to the numerical values that were then employed as computed translations to calculate factor weights for correct mapping. The main objective of the AHP framework is to score the weight of each LSZ determining factor. The quality of the outcome was highly discretionary because of the subjective nature of pair-wise comparisons. Due to several paths on which the relative relevance of components was appraised, the level of consistency was employed in making the judgments. The weights of

LSZ parameters such as ‘Dd’, ‘Dt’, ‘DI’, ‘In’, ‘Fs’, ‘Lo’, ‘Jf’, ‘Be’, ‘St’, ‘Di’, ‘Ri’, ‘Rr’, ‘Sl’, ‘As’, ‘Lg’, and ‘Ld’ are summarized in the pair-wise comparison matrix (Table 3 and Table 4). Here, normalized weights were assigned and rank given to each sub-classes. The consistency ratio (CR) was defined as the ratio between the consistency index and the random consistency index (Mukherjee and Singh 2020). The inconsistency is permitted if the consistency ratio is less than or equal to 0.1 but, if the consistency ratio is larger than 0.1, the subjective judgment must be revised. The CR is expressed as:

$$CR = \frac{CI}{RCI}, \quad (8)$$

where, RCI = the random consistency index, and CI = consistency index, which can be expressed as follows:

$$CI = \frac{\lambda_{max} - n}{n - 1}, \quad (9)$$

where, λ_{max} = the biggest particular value in the matrix, and $n - 1$ = the matrix's order. The RCI value was depicted in Table 5 based on Saaty (1990). The CR is scaled from 0 to 1, where 1 indicates the chance of a randomly produced matrix and CR less than 0.10 indicates a reasonable level of homogeneity (Malczewski 2006). The resulting weights are shown in Table 6 with an acceptable CR. As the linear weighted combination computation rule, weights should add up to 1.0, i.e.,

$$\sum_{j=1}^n w_j = 1. \quad (10)$$

[Table 2 Saaty’s (2005) scale of relative importance]

[Table 3 Pair-wise comparison matrix of nine selected parameters for preparing relief diversity map]

[Table 4 Pair-wise comparison matrix of seven selected parameters for preparing drainage diversity map]

[Table 5 Random consistency index (RCI) based on Saaty (1990)]

[Table 6 Normalized weight for all parameters based on AHP and rank given to their sub-classes based on landslide vulnerability]

2.3. Validation of the work

Validation of the LSZ is required for the scientific significance and utility of the study. The final LSZ of the present study area has been validated through systematic validation processes. In the first step, validation is done by computing the frequency density of landslides with the landslide occurrences data of the GSI. In the second step, the final map is validated by preparing the ROC-AUC. This ROC-AUC has been prepared in ArcGIS software using the 'ArcSDM' tool. It is a helpful tool used to validate the final susceptibility map of such kinds of studies.

3. Results and discussion

3.1. Relief diversity (RD) of the basin

The relief diversity (RD) represents the vulnerability of the study area based on terrain properties and slope instability (Basu and Pal 2019). It has been produced in respect of nine parameters, viz. 'Be', 'Rr', 'Di', 'Ri', 'Sl', 'As', 'Lg', 'Ld', and 'St' of the basin. The produced map was categorized into five successive zones, i.e., 'very low' (2.40%), 'low' (34.02%), 'moderate' (45.01%), 'high' (18.01%), and 'very high' (0.56%), as illustrated in Fig. 5 (a). In this vulnerability indicator, the 'moderate' zone bears the highest area, while the 'very high' zone bears the lowest area and is found in the southwestern part of the basin. Basically, in terms of the condition of the terrain, the 'very high' relief diversity zone is most vulnerable, and the 'very low' zone is least vulnerable, occupied in the lower section of the basin.

[Fig. 5 (a) Relief diversity and (b) Drainage diversity maps of the Ragnu Khola River Basin in the Darjeeling Himalaya]

3.2. Drainage diversity (DD) of the basin

The drainage diversity (DD) of the basin is portrayed based on the strength of the properties of the drainages (Basu and Pal 2019). It results from the 'Fs', 'Dd', 'Dt', 'DI', 'Lo', 'Jf', and 'In'. The spatial distribution of the DD is displayed in Fig. 5 (b), and it is also categorized in five classes, viz., 'very low', 'low', 'moderate', 'high', 'very high'. The 'very high' DD is mainly found in the upper part of the region, and it has been successively low towards the lower reaches. The 'very high' zone is characterized by steep sloping land, high drainage density, high stream frequency, and vice-versa. The 'low' DD zone occupies the maximum area (45.54%) of the basin, while the 'very high' zone occupies the minimum extent (5.07%). The 'moderate' DD zone covered 25.98% area, the 'very low' DD zone covered 14.01% area, and the 'high' DD zone covered 9.40% area of the region.

3.3. Landslide susceptibility zones (LSZ)

The landslide susceptibility mapping (LSM) of the Ragnu Khola River Basin was prepared using the AHP MCDM method based on 16 morphometric parameters. In this study, mainly LSM is related to the morphometric characteristics of the river. It represents the vulnerability of the region in relation to relief and drainage conditions (Basu and Pal 2019). The LSM is displayed in Fig. 6 with five distinct zones. The zones are categorized using the natural break classification technique (Achour et al. 2017), viz. 'very low', 'low', 'moderate', 'high', and 'very high'. The 'moderate' susceptible zone contains most of the area (47.70%) of the region, followed by 'low' zone (31.70%), 'high' zone (17.83%), 'very high' zone (1.45%), and 'very low' zone (1.32%).

The spatial distribution pattern demonstrates that the occurrences of landslides have been decreasing from the upper part to the lower part of the basin, i.e., from the southwest to the northeast corner of the map. Therefore, the upper catchment is very highly susceptible to the landslides hazards. The 'very high' zone is associated with highly elevated land, bearing 1820 to 2478 m in height. The region is also represented high 'Dd' (5.63 to 7.15 km/km²), maximum 'Jf' (10.39 to 12.99) and 'Fs' (13 to 24 streams/km²), and highly rugged topography. Geologically, the zones range from 'very high' to 'moderate' landslide susceptibility are situated over the Kanchenjunga Gneiss formation and high lineament density zone (0.79 to 1.83 km/km²). The 'high' susceptible areas are most vulnerable in terms of both DD and RD. Here, the rate of soil erosion is high due to extreme DD and RD, and the region is not suitable for agricultural and constructional activities (Pal and Saha 2017). The Chungthang and Gorubathan formation are less susceptible to landslides in the basin. The 'low' and 'very low' susceptible areas are less in terms of 'Dd' (1.84 to 4.07 km/km²), ruggedness (0 to 1.13), and 'Rr' (140 to 443 m). These zones are often found between 230 to 722 m altitudes, with 'Ld' ranging from 0 to 0.28 km/km².

[Fig. 6 Landslide susceptibility zones in the Ragnu Khola River Basin of Darjeeling Himalaya]

3.4. Validation

Based on the landslide occurrence data of the study area, the authors have been computed the frequency density of landslides (FDL) (Basu and Pal 2019), as illustrated in Table 7. The 'very high' (2.19/km²) FDL is associated with the 'very high' LSZ. The 'high' (0.80/km²) FDL area is also found for the 'high' LSZ. In comparison, the 'moderate' (0.36/km²) FDL actually falls in

the moderate 'LSZ'. 'Very low' LSZ indicates no landslide point due to the FDL is zero. The second method entails creating a ROC for verification of the LSZ. The landslide occurrence point data of GSI and landslide susceptibility layer are considered when generating the ROC curve. The outcome reveals 0.721, i.e., 72.10% area under the curve (AUC) (Fig. 7). The result implies a fair accuracy rate as it falls between 0.70 to 0.80 (Rasyid et al. 2016). Therefore, all the morphometric indicators are acceptable in determining the landslide susceptibility model of the Ragnu Khola Basin. The google earth images of landslide prone areas also manifest in Fig. 8, mainly dominating in the 'high' to 'very high' LSZ.

[Table 7 Frequency density of landslide (FDL) occurrences in different landslide susceptibility zones]

[Fig. 7 ROC curve for validation of the landslide susceptibility zones]

4. Conclusion

The landslide susceptibility mapping (LSM) of the Ragnu Khola River Basin in Darjeeling Himalaya included a variety of morphometric criteria, and these criteria were also divided into two-part, such as drainage diversity (DD) and relief diversity (RD) indicators. These morphometric parameters reflect the characteristics of the hydro-geomorphological system of the study area. It was observed during the study that morphometric parameters are capable of creating the landslide susceptibility map. The study region is only about 64.79 km² in its extent, and the morphometric variables are reliable even this small-scale perspective for identifying landslide susceptibility zones (LSZ). Aside from that, morphometric parameters show that areas with higher drainage density and cliffs are primarily vulnerable to landslide phenomena in the river basin. Almost monsoon rains cause landslides in these places every year. The resulting map has provided the spatial distribution of landslide zones, and the FDL and ROC curve analysis validated it. It was come out from the study that a high LSZ is interrelated to the places particularly vulnerable in drainage and relief conditions. The upper catchment of the basin is very sensitive and varies from high to very high landslide zones, while the lower part is less vulnerable. There 17.83% area is highly susceptible to landslides, which are observed in the upper catchment of the basin. Therefore, there should be implemented restrictions and proper guidelines for constructional activity. Thus, the MCDM technique is useful globally to generate such a kind of susceptibility map. The work will also assist the decision-makers in

developing strategies to prevent landslide destruction. This type of work will be required in the future for appropriate planning of developmental activities in tectonically active areas.

Acknowledgements

The authors would like to express cordial thanks to the Geography and Applied Geography Department, University of North Bengal, for infrastructural support into the work. The authors will also be thankful to the GSI, SOI, NBSS & LUP, and USGS for providing the required data and map related to the study.

Authors' contributions

All authors wrote the manuscript and developed the research methodology. All authors also read and approved the final manuscript.

Funding

No funding was received for this work.

Availability of data and materials

Topographical map was received from Survey of India (SOI) which freely available from <https://soinakshe.uk.gov.in> website. Landsat images and DEM will freely be availed from <https://earthexplorer.usgs.gov/> website. Soil map was collected from National Bureau of Soil Survey and Land Use Planning (NBSS & LUP). Geological map was taken from Geological Survey of India (GSI).

Competing interests

The authors declare that they have no competing interests.

References

- Achour Y, Boumezbeur A, Hadji R, Chouabbi A., Cavaleiro V, Bendaoud EA (2017) Landslide susceptibility mapping using analytic hierarchy process and information value methods along a highway road section in Constantine, Algeria. *Arabian Journal of Geosciences*, 10(8), p.194. DOI: <https://doi.org/10.1007/s12517-017-2980-6>.
- Agarwal CS (1998) Study of drainage pattern through aerial data in Naugarh area of Varanasi district, UP. *Journal of the Indian Society of Remote Sensing*, 26(4), 169-175. DOI: <https://doi.org/10.1007/BF02990795>.

Ahmadlou M, Karimi M, Alizadeh S, Shirzadi A, Parvinnejhad D, Shahabi H, Panahi M (2019) Flood susceptibility assessment using integration of adaptive network-based fuzzy inference system (ANFIS) and biogeography-based optimization (BBO) and BAT algorithms (BA). *Geocarto International*, 34(11), pp.1252-1272. DOI: <https://doi.org/10.1080/10106049.2018.1474276>.

Altın TB, Gökkaya E (2018) Assessment of landslide-triggering factors and occurrence using morphometric parameters in Geyraz Basin, Tokat, Northern Turkey. *Environmental earth sciences*, 77(4), pp.1-20. DOI: <https://doi.org/10.1007/s12665-018-7315-8>.

Arabameri A, Pourghasemi HR, Yamani M (2017) Applying different scenarios for landslide spatial modeling using computational intelligence methods. *Environmental Earth Sciences*, 76(24), pp.1-20. DOI: <https://doi.org/10.1007/s12665-017-7177-5>.

Arabameri A, Pradhan B, Rezaei K, Sohrabi M, Kalantari Z (2019) GIS-based landslide susceptibility mapping using numerical risk factor bivariate model and its ensemble with linear multivariate regression and boosted regression tree algorithms. *Journal of Mountain Science*, 16(3), pp.595-618. DOI: <https://doi.org/10.1007/s11629-018-5168-y>.

Ayalew L, Yamagishi H (2005) The application of GIS-based logistic regression for landslide susceptibility mapping in the Kakuda-Yahiko Mountains, Central Japan. *Geomorphology*, 65(1-2), pp.15-31. DOI: <https://doi.org/10.1016/j.geomorph.2004.06.010>.

Bahrami Y, Hassani H, Maghsoudi A (2021) Landslide susceptibility mapping using AHP and fuzzy methods in the Gilan province, Iran. *GeoJournal*, 86(4), pp.1797-1816. DOI: <https://doi.org/10.1007/s10708-020-10162-y>.

Basu T, Pal S (2018) Identification of landslide susceptibility zones in Gish River basin, West Bengal, India. *Georisk: Assessment and Management of Risk for Engineered Systems and Geohazards*, 12(1), 14-28. DOI: <https://doi.org/10.1080/17499518.2017.1343482>.

Basu T, Pal S (2019) RS-GIS based morphometrical and geological multi-criteria approach to the landslide susceptibility mapping in Gish River Basin, West Bengal, India. *Advances in Space Research*, 63(3), pp.1253-1269. DOI: <https://doi.org/10.1016/j.asr.2018.10.033>.

Bennie J, Hill MO, Baxter R, Huntley B (2006) Influence of slope and aspect on long-term vegetation change in British chalk grasslands. *Journal of ecology*, 94(2), pp.355-368. DOI: <https://doi.org/10.1111/j.1365-2745.2006.01104.x>.

Beullens J, Van de Velde D, Nyssen J (2014) Impact of slope aspect on hydrological rainfall and on the magnitude of rill erosion in Belgium and northern France. *Catena*, 114, pp.129-139. DOI: <https://doi.org/10.1016/j.catena.2013.10.016>.

Bhattacharya SK (2013) The study of Paglajhora landslide in the Darjeeling Hills, West Bengal, India. *Ind. J. Spat. Sci.* 4.0 (1), 21–27.

Chamling M (2013) Landslides: a geographical review in and around Pagla Jhora Region of the Eastern Himalayan belt of Darjeeling, West Bengal, *Peripex-Indian Journal of Research*, 2(8), 131-133.

Chen W, Xie X, Wang J, Pradhan B, Hong H, Bui DT, Duan Z, Ma J (2017) A comparative study of logistic model tree, random forest, and classification and regression tree models for spatial prediction of landslide susceptibility. *Catena*, 151, pp.147-160. DOI: <https://doi.org/10.1016/j.catena.2016.11.032>.

Chen W, Shahabi H, Shirzadi A, Hong H, Akgun A, Tian Y, Liu J, Zhu AX, Li S (2019) Novel hybrid artificial intelligence approach of bivariate statistical-methods-based kernel logistic regression classifier for landslide susceptibility modeling. *Bulletin of Engineering Geology and the Environment*, 78(6), pp.4397-4419. DOI: <https://doi.org/10.1007/s10064-018-1401-8>.

Chu L, Wang LJ, Jiang J, Liu X, Sawada K, Zhang J (2019) Comparison of landslide susceptibility maps using random forest and multivariate adaptive regression spline models in combination with catchment map units. *Geosciences Journal*, 23(2), pp.341-355. DOI: <https://doi.org/10.1007/s12303-018-0038-8>.

Clarke JI (1996) *Morphometry from maps. Essays in geomorphology.*

Crawford MM, Dortch JM, Koch HJ, Killen AA, Zhu J, Zhu Y, Bryson LS, Haneberg WC (2021) Using landslide-inventory mapping for a combined bagged-trees and logistic-regression approach to determining landslide susceptibility in eastern Kentucky, United States. *Quarterly Journal of Engineering Geology and Hydrogeology*. DOI: <https://doi.org/10.1144/qjegh2020-177>.

Das G, Lepcha K (2019) Application of logistic regression (LR) and frequency ratio (FR) models for landslide susceptibility mapping in Relli Khola river basin of Darjeeling Himalaya, India. *SN Applied Sciences*, 1(11), pp.1-22. DOI: <https://doi.org/10.1007/s42452-019-1499-8>.

Dou J, Yamagishi H, Zhu Z, Yunus AP, Chen CW (2018) TXT-tool 1.081-6.1 A comparative study of the binary logistic regression (BLR) and artificial neural network (ANN) models for GIS-based spatial predicting landslides at a regional scale. In *Landslide dynamics: ISDR-ICL landslide interactive teaching tools* (pp. 139-151). Springer, Cham. DOI: https://doi.org/10.1007/978-3-319-57774-6_10.

Erener A, Düzgün HSB (2010) Improvement of statistical landslide susceptibility mapping by using spatial and global regression methods in the case of More and Romsdal (Norway). *Landslides*, 7(1), pp.55-68. DOI: <https://doi.org/10.1007/s10346-009-0188-x>.

Faniran A (1968) The index of drainage intensity: a provisional new drainage factor. *Aust J Sci*, 31(9), pp.326-330.

Gayen S, Bhunia GS, Shit PK (2013) Morphometric analysis of Kangshabati-Darakeswar Interfluvies area in West Bengal, India using ASTER DEM and GIS techniques. *J Geol Geosci*, 2(4), 1-10. DOI: 10.4172/2329-6755.1000133.

Gorokhovich Y, Vustianiuk A (2021) Implications of slope aspect for landslide risk assessment: a case study of Hurricane Maria in Puerto Rico in 2017. *Geomorphology*, p.107874. DOI: <https://doi.org/10.1016/j.geomorph.2021.107874>.

Gu T, Li J, Wang M, Duan P (2021) Landslide susceptibility assessment in Zhenxiong County of China based on geographically weighted logistic regression model. *Geocarto International*, pp.1-23. DOI: <https://doi.org/10.1080/10106049.2021.1903571>.

Hasegawa S, Nonomura A, Nakai S, Dahal RK (2014) Drainage density as rainfall induced landslides susceptibility index in small catchment area. *International Journal of Landslide and Environment*, 1(1), pp.27-28.

Hong H, Panahi M, Shirzadi A, Ma T, Liu J, Zhu AX, Chen W, Kougias I, Kazakis N (2018) Flood susceptibility assessment in Hengfeng area coupling adaptive neuro-fuzzy inference system with genetic algorithm and differential evolution. *Science of the total Environment*, 621, pp.1124-1141. DOI: <https://doi.org/10.1016/j.scitotenv.2017.10.114>.

Horton RE (1932) Drainage-basin characteristics. *Eos, transactions american geophysical union*, 13(1), 350-361. DOI: <https://doi.org/10.1029/TR013i001p00350>.

Horton RE (1945) Erosional development of streams and their drainage basins; hydrophysical approach to quantitative morphology. *Bull. Geol. Soc. Am.* 56, 275–370.

Hurtrez JE, Sol C, Lucazeau F (1999) Effect of drainage area on hypsometry from an analysis of small-scale drainage basins in the Siwalik Hills (Central Nepal). *Earth Surface Processes and Landforms: The Journal of the British Geomorphological Research Group*, 24(9), 799-808. DOI: [https://doi.org/10.1002/\(SICI\)1096-9837\(199908\)24:9<799::AID-ESP12>3.0.CO;2-4](https://doi.org/10.1002/(SICI)1096-9837(199908)24:9<799::AID-ESP12>3.0.CO;2-4).

Iqbal J, Cui PENG, Hussain ML, Pourghasemi HR, Cheng DQ, Shah SU, Pradhan B (2021) Landslide susceptibility assessment along the Dubair-Dudishal section of the Karakoram highway, northwestern Himalayas, Pakistan. *Acta Geodynamica et Geomaterialia*, 18(2), pp.137-155. DOI: 10.13168/AGG.2021.0010.

Jacynth Jennifer J, Saravanan S (2021) Artificial neural network and sensitivity analysis in the landslide susceptibility mapping of Idukki district, India. *Geocarto International*, pp.1-23. DOI: <https://doi.org/10.1080/10106049.2021.1923831>.

Kale VS, Gupta A (2001) *Introduction to Geomorphology*. Orient Blackswan Private Limited.

Kaur H, Gupta S, Parkash S, Thapa R (2018) Knowledge-driven method: A tool for landslide susceptibility zonation (LSZ). *Geology, Ecology, and Landscapes*, pp.1-15. DOI: <https://doi.org/10.1080/24749508.2018.1558024>.

Kaur L, Rishi MS, Singh G, Thakur SN (2020) Groundwater potential assessment of an alluvial aquifer in Yamuna sub-basin (Panipat region) using remote sensing and GIS techniques in conjunction with analytical hierarchy process (AHP) and catastrophe theory (CT). *Ecological Indicators*, 110, p.105850. DOI: <https://doi.org/10.1016/j.ecolind.2019.105850>.

Keefer DK, Larsen MC (2007) Assessing landslide hazards. *Science*, pp.1136-1138.

Liu Z, Gilbert G, Cepeda JM, Lysdahl AOK, Piciullo L, Hefre H, Lacasse S (2021) Modelling of shallow landslides with machine learning algorithms. *Geoscience Frontiers*, 12(1), pp.385-393. DOI: <https://doi.org/10.1016/j.gsf.2020.04.014>.

Lucchese LV, de Oliveira GG, Pedrollo OC (2021) Mamdani fuzzy inference systems and artificial neural networks for landslide susceptibility mapping. *Natural Hazards*, 106(3), pp.2381-2405.

Luo Y, He SM, Chen FZ, Li XP, He JC (2015) A physical model considered the effect of overland water flow on rainfall-induced shallow landslides. *Geoenvironmental Disasters*, 2(1), pp.1-11. DOI: <https://doi.org/10.1186/s40677-015-0017-6>.

Malczewski J (2006) GIS-based multi-criteria decision analysis: a survey of the literature. *International journal of geographical information science*, 20(7), pp.703-726. DOI: <https://doi.org/10.1080/13658810600661508>.

Manaouch M, Mohamed S, Imad F (2021) Coupling Fuzzy logic and Analytical Hierarchy Process (FAHP) with GIS for Landslide Susceptibility Mapping (LSM) in Ziz upper watershed, SE Morocco.

Mandal S, Maiti R (2014) Role of lithological composition and lineaments in Landsliding: a case study of Shivkhola Watershed, Darjeeling Himalaya. *Int J Geol Earth Environ Sci*, 4(1), 126-132.

Mondal S, Mandal S (2019) Landslide susceptibility mapping of Darjeeling Himalaya, India using index of entropy (IOE) model. *Applied Geomatics*, 11(2), pp.129-146. DOI: <https://doi.org/10.1007/s12518-018-0248-9>.

Mukherjee I, Singh UK (2020) Delineation of groundwater potential zones in a drought-prone semi-arid region of east India using GIS and analytical hierarchical process techniques. *Catena*, 194, p.104681. DOI: <https://doi.org/10.1016/j.catena.2020.104681>.

Nad C (2015) Landslide Hazard Management of Darjeeling Hill-A Critical Need for Inhabited. *International Journal of Humanities and Social Science Invention*, 4(3), 48-60.

Nadim F, Kjekstad O (2009) Assessment of global high-risk landslide disaster hotspots. In *Landslides–Disaster Risk Reduction* (pp. 213-221). Springer, Berlin, Heidelberg. DOI: https://doi.org/10.1007/978-3-540-69970-5_11.

Nanehkaran YA, Mao Y, Azarafza M, Kockar MK, Zhu HH (2021) Fuzzy-based multiple decision method for landslide susceptibility and hazard assessment: A case study of Tabriz, Iran. *Geomechanics and Engineering*, 24(5), pp.407-418. DOI: <https://doi.org/10.12989/gae.2021.24.5.407>.

Navarro IJ, Yepes V, Martí JV (2019) A review of multi-criteria assessment techniques applied to sustainable infrastructure design. *Advances in civil engineering*, 2019. DOI: <https://doi.org/10.1155/2019/6134803>.

Nir D (1957) The ratio of relative and absolute altitudes of Mt. Carmel: a contribution to the problem of relief analysis and relief classification. *Geographical Review*, 47(4), pp.564-569.

Pal S, Saha TK (2017) Exploring drainage/relief-scape sub-units in Atreyee river basin of India and Bangladesh. *Spatial Information Research*, 25(5), pp.685-692. DOI: <https://doi.org/10.1007/s41324-017-0133-3>.

Petley D (2012) Global patterns of loss of life from landslides. *Geology*, 40(10), pp.927-930. DOI: <https://doi.org/10.1130/G33217.1>.

Patton PC, Baker VR (1976) Morphometry and floods in small drainage basins subject to diverse hydrogeomorphic controls. *Water resources research*, 12(5), pp.941-952. DOI: <https://doi.org/10.1029/WR012i005p00941>.

Pham QB, Achour Y, Ali SA, Parvin F, Vojtek M, Vojteková J, Al-Ansari N, Achu AL, Costache R, Khedher KM, Anh DT (2021) A comparison among fuzzy multi-criteria decision making, bivariate, multivariate and machine learning models in landslide susceptibility mapping. *Geomatics, Natural Hazards and Risk*, 12(1), pp.1741-1777. DOI: <https://doi.org/10.1080/19475705.2021.1944330>.

Pourghasemi HR, Mohammady M, Pradhan B (2012a) Landslide susceptibility mapping using index of entropy and conditional probability models in GIS: Safarood Basin, Iran. *Catena*, 97, pp.71-84. DOI: <https://doi.org/10.1016/j.catena.2012.05.005>.

Pourghasemi HR, Pradhan B, Gokceoglu C (2012b) Application of fuzzy logic and analytical hierarchy process (AHP) to landslide susceptibility mapping at Haraz watershed, Iran. *Natural hazards*, 63(2), pp.965-996. DOI: <https://doi.org/10.1007/s11069-012-0217-2>.

Rasyid AR, Bhandary NP, Yatabe R (2016) Performance of frequency ratio and logistic regression model in creating GIS based landslides susceptibility map at Lompobattang Mountain, Indonesia. *Geoenvironmental Disasters*, 3(1), 1-16. DOI: <https://doi.org/10.1186/s40677-016-0053-x>.

Reddy GPO, Maji AK, Gajbhiye KS (2004) Drainage morphometry and its influence on landform characteristics in a basaltic terrain, Central India—a remote sensing and GIS approach. *International Journal of Applied Earth Observation and Geoinformation*, 6(1), 1-16. DOI: <https://doi.org/10.1016/j.jag.2004.06.003>.

Saaty TL (1990) An exposition of the AHP in reply to the paper “remarks on the analytic hierarchy process”. *Management science*, 36(3), pp.259-268. DOI: <https://doi.org/10.1287/mnsc.36.3.259>.

Saaty TL (2004) Fundamentals of the analytic network process—multiple networks with benefits, costs, opportunities and risks. *Journal of systems science and systems engineering*, 13(3), pp.348-379. DOI: <https://doi.org/10.1007/s11518-006-0171-1>.

Saaty TL (2005) Analytic hierarchy process. *Encyclopedia of biostatistics*.

Saaty TL (2008) Decision making with the analytic hierarchy process. *International journal of services sciences*, 1(1), pp.83-98.

Saha AK, Gupta RP, Arora MK (2002) GIS-based landslide hazard zonation in the Bhagirathi (Ganga) valley, Himalayas. *International journal of remote sensing*, 23(2), 357-369. DOI: <https://doi.org/10.1080/01431160010014260>.

Sahana M, Sajjad H (2017) Evaluating effectiveness of frequency ratio, fuzzy logic and logistic regression models in assessing landslide susceptibility: a case from Rudraprayag district, India. *Journal of Mountain Science*, 14(11), pp.2150-2167. DOI: <https://doi.org/10.1007/s11629-017-4404-1>.

Saleem N, Huq M, Twumasi NYD, Javed A, Sajjad A (2019) Parameters derived from and/or used with digital elevation models (DEMs) for landslide susceptibility mapping and landslide risk assessment: a review. *ISPRS International Journal of Geo-Information*, 8(12), p.545. DOI: <https://doi.org/10.3390/ijgi8120545>.

Sarkar S, Kanungo DP (2004) An integrated approach for landslide susceptibility mapping using remote sensing and GIS. *Photogrammetric Engineering & Remote Sensing*, 70(5), pp.617-625. DOI: <https://doi.org/10.14358/PERS.70.5.617>.

Sarkar S, Kanungo DP, Mehrotra GS (1995) Landslide hazard zonation: a case study in Garhwal Himalaya, India. *Mountain Research and Development*, 301-309.

Schumm SA (1956) Evolution of drainage systems and slopes in badlands at Perth Amboy, New Jersey. *Geological society of America bulletin*, 67(5), pp.597-646. DOI: [https://doi.org/10.1130/0016-7606\(1956\)67\[597:EODSAS\]2.0.CO;2](https://doi.org/10.1130/0016-7606(1956)67[597:EODSAS]2.0.CO;2).

Sharma LP, Patel N, Debnath P, Ghose MK (2012) Assessing landslide vulnerability from soil characteristics—a GIS-based analysis. *Arabian Journal of Geosciences*, 5(4), pp.789-796. DOI: <https://doi.org/10.1007/s12517-010-0272-5>.

Shirzadi A, Shahabi H, Chapi K, Bui DT, Pham BT, Shahedi K, Ahmad BB (2017) A comparative study between popular statistical and machine learning methods for simulating volume of landslides. *Catena*, 157, 213-226. DOI: <https://doi.org/10.1016/j.catena.2017.05.016>.

Smith GH (1935) The relative relief of Ohio. *Geographical review*, 25(2), pp.272-284.

Strahler AN (1952) Hypsometric (area-altitude) analysis of erosional topography. *Geological society of America bulletin*, 63(11), 1117-1142. DOI: [https://doi.org/10.1130/0016-7606\(1952\)63\[1117:HAAOET\]2.0.CO;2](https://doi.org/10.1130/0016-7606(1952)63[1117:HAAOET]2.0.CO;2).

Strahler AN (1956) Quantitative slope analysis. *Geological Society of America Bulletin*, 67(5), pp.571-596. DOI: [https://doi.org/10.1130/0016-7606\(1956\)67\[571:QSA\]2.0.CO;2](https://doi.org/10.1130/0016-7606(1956)67[571:QSA]2.0.CO;2).

Strahler AN (1964) Part II. Quantitative geomorphology of drainage basins and channel networks. *Handbook of Applied Hydrology*: McGraw-Hill, New York, 4-39.

Sujatha ER, Sridhar V (2021) Landslide susceptibility analysis: a logistic regression model case study in Coonoor, India. *Hydrology*, 8(1), p.41. DOI: <https://doi.org/10.3390/hydrology8010041>.

Varnes DJ (1984) *Landslide hazard zonation: a review of principles and practice*. UNESCO, Paris, pp. 1-63.

Virdi NS, Sah MP, Bartarya SK (1997) Mass wasting, its manifestations, causes and control: some case histories from Himachal Himalaya. *Perspectives of mountain risk engineering in the Himalayan Region*. Gyanodaya Prakashan, Nainital, 111-130.

Wang G, Lei X, Chen W, Shahabi H, Shirzadi A (2020) Hybrid computational intelligence methods for landslide susceptibility mapping. *Symmetry*, 12(3), p.325. DOI: <https://doi.org/10.3390/sym12030325>.

White GF (1974) *Natural hazards, local, national, global*. Oxford University Press.

Zarei E, Ramavandi B, Darabi AH, Omidvar M, (2021) A framework for resilience assessment in process systems using a fuzzy hybrid MCDM model. *Journal of Loss Prevention in the Process Industries*, 69, p.104375. DOI: <https://doi.org/10.1016/j.jlp.2020.104375>.

Zavoianc I (1985) *Morphometry of drainage basins (development in water science)*. Publisher: Elsevier science, 20, pp.104-105.

Zhou S, Zhang Y, Tan X, Abbas SM (2021) A comparative study of the bivariate, multivariate and machine-learning-based statistical models for landslide susceptibility mapping in a seismic-prone region in China. *Arabian Journal of Geosciences*, 14(6), pp.1-19. DOI: <https://doi.org/10.1007/s12517-021-06630-5>.

Figures

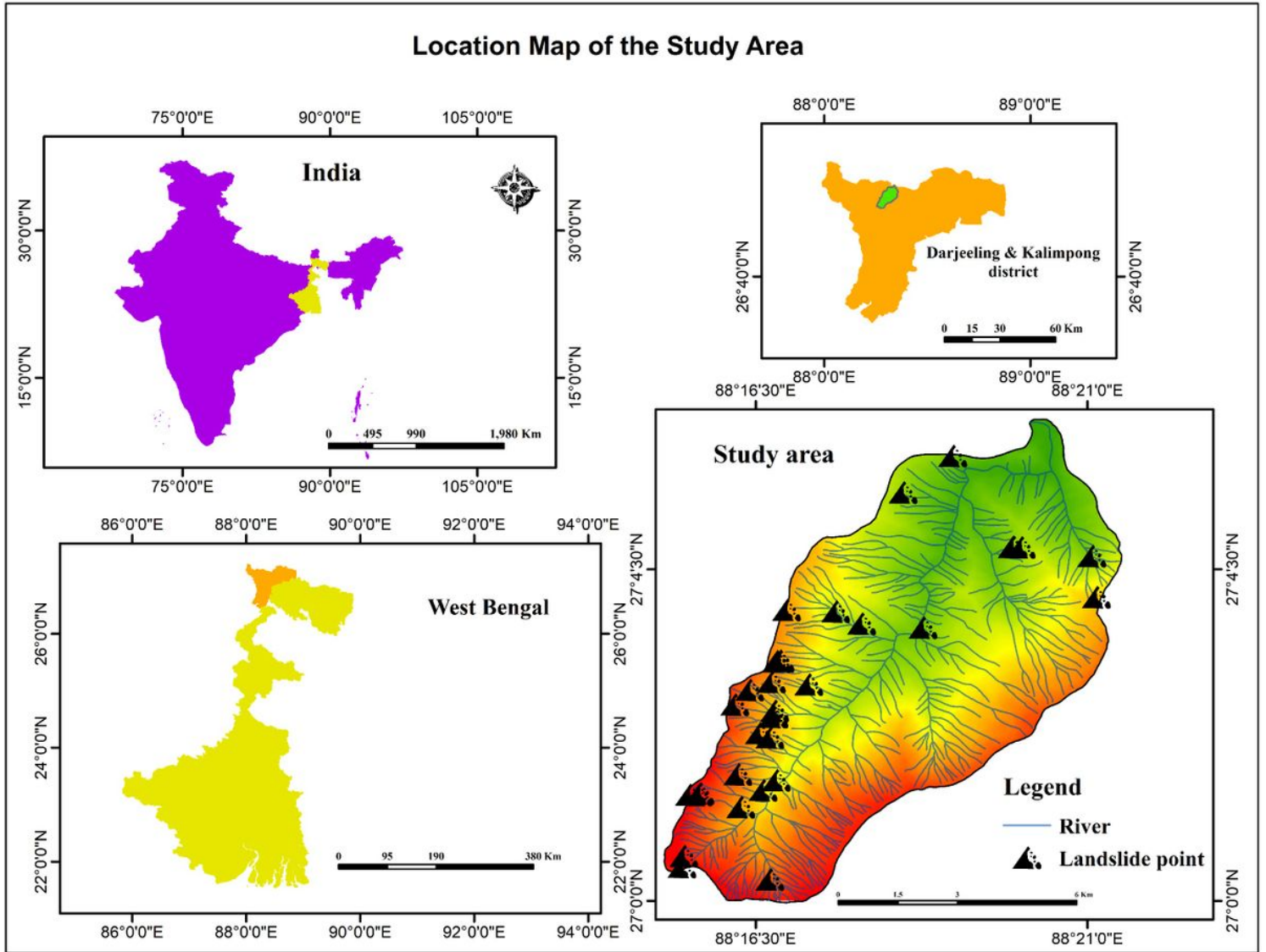


Figure 1

Location map of the Ragnu Khola River Basin in the Darjeeling Himalaya

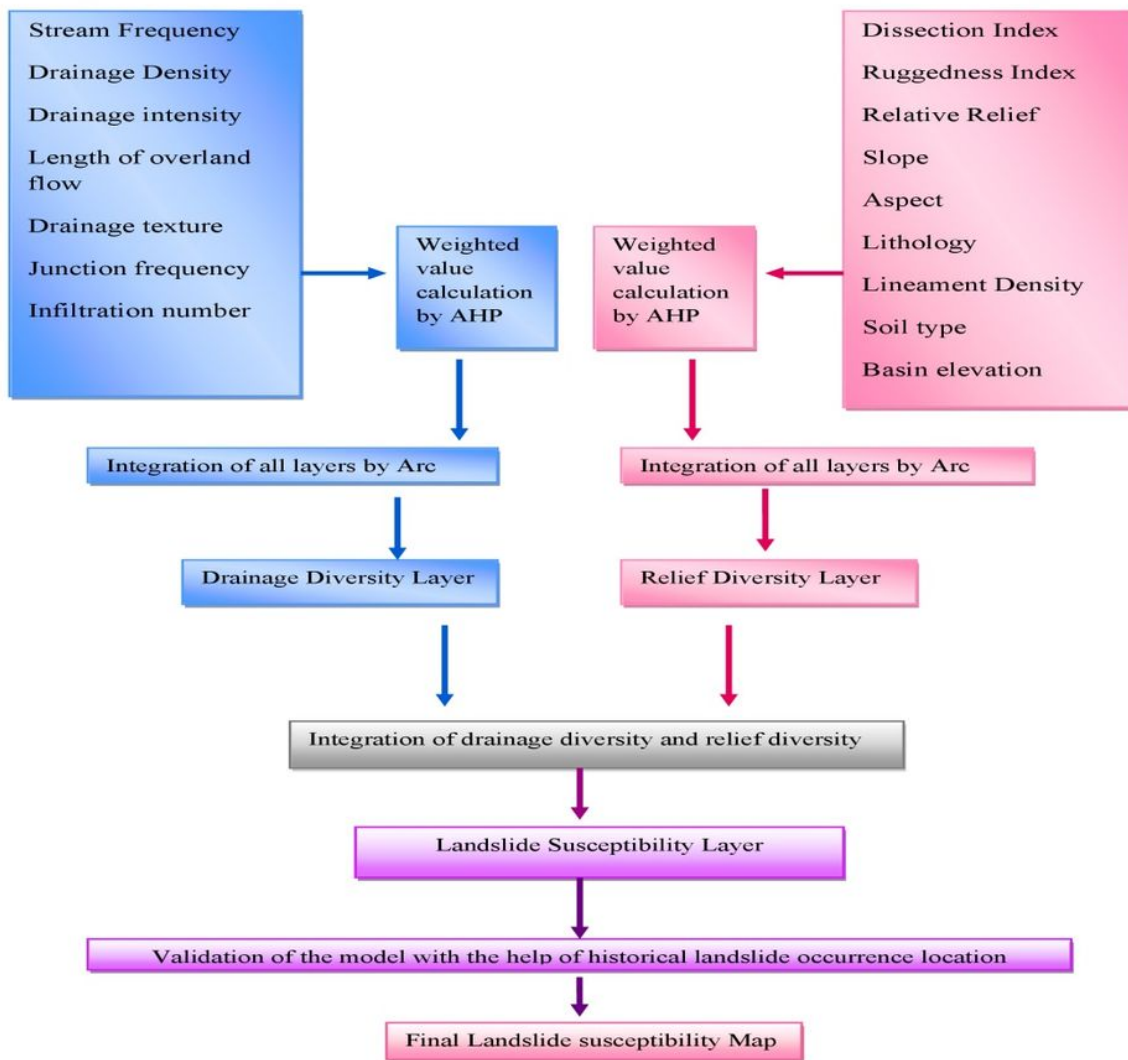


Figure 2

Methodological framework of the present study

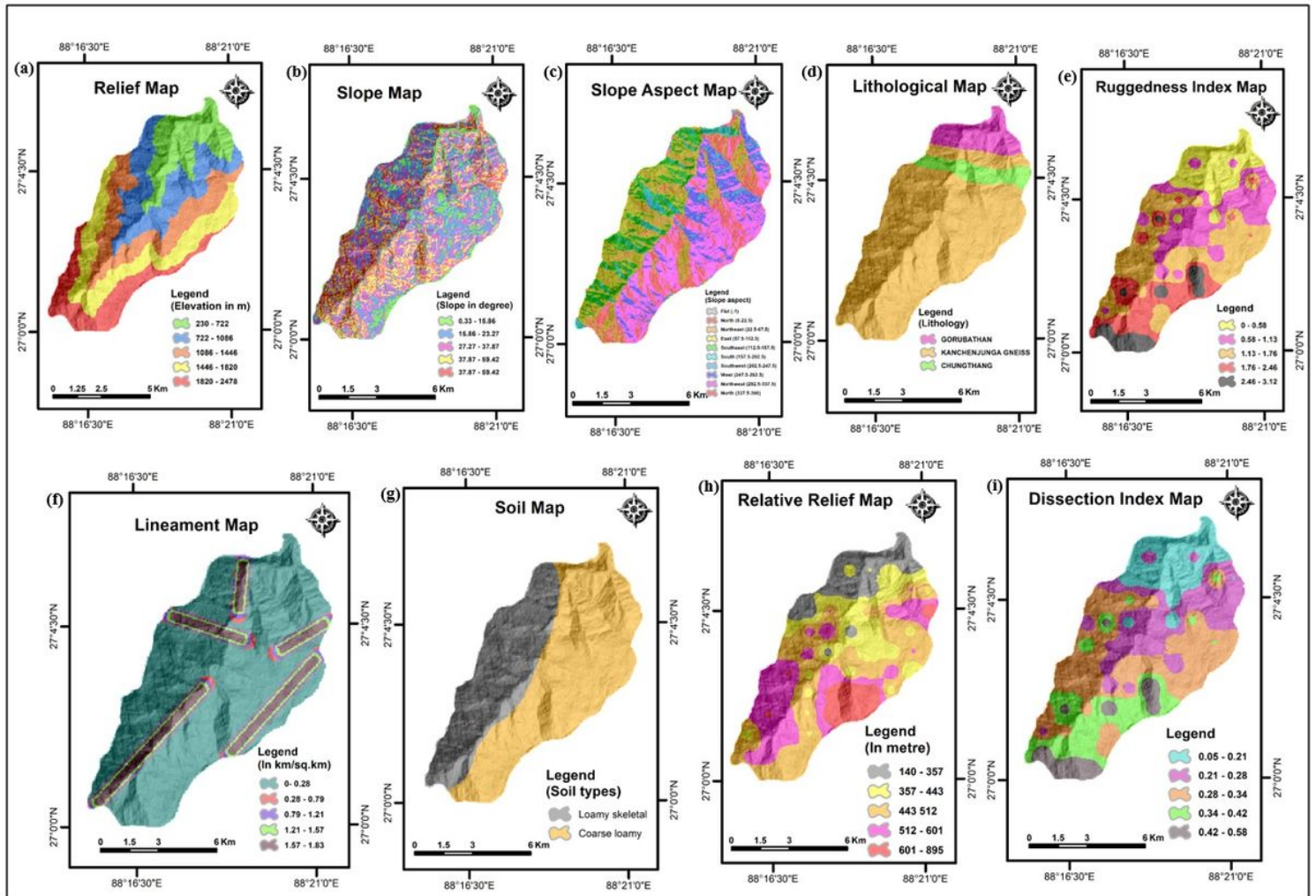


Figure 3

Raster maps of different relief diversity parameters (a) Basin relief, (b) Slope, (c) Slope aspect, (d) Lithological formation, (e) Ruggedness index, (f) Lineament density, (g) Soil type, (h) Relative relief, and (i) Dissection index of the Ragnu Khola River Basin in the Darjeeling Himalaya

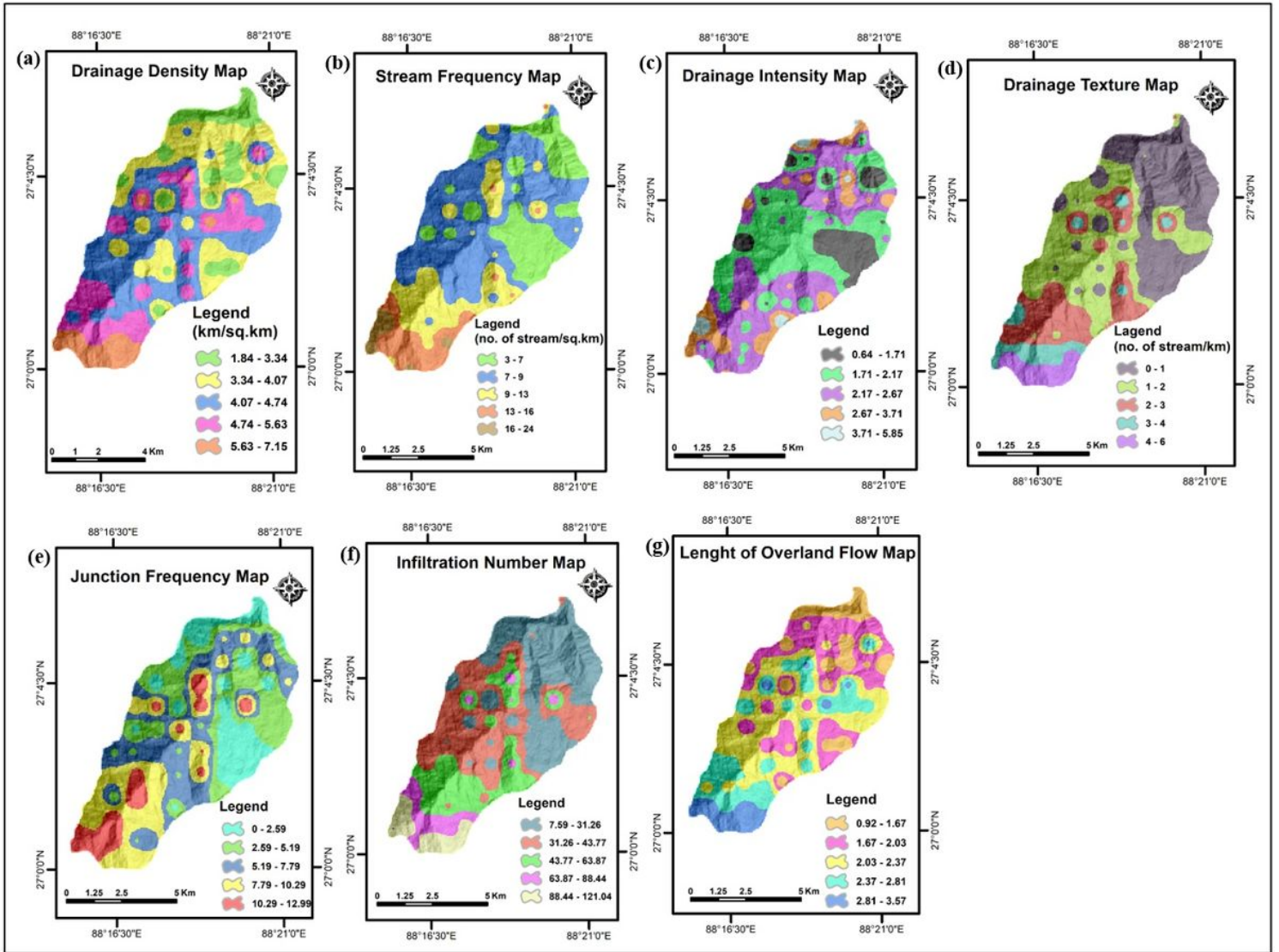


Figure 4

Raster maps of different drainage diversity parameters (a) Drainage density, (b) Stream frequency, (c) Drainage intensity, (d) Drainage texture, (e) Junction frequency, (f) Infiltration number, and (g) Length of overland flow of the Ragnu Khola River Basin in the Darjeeling Himalaya

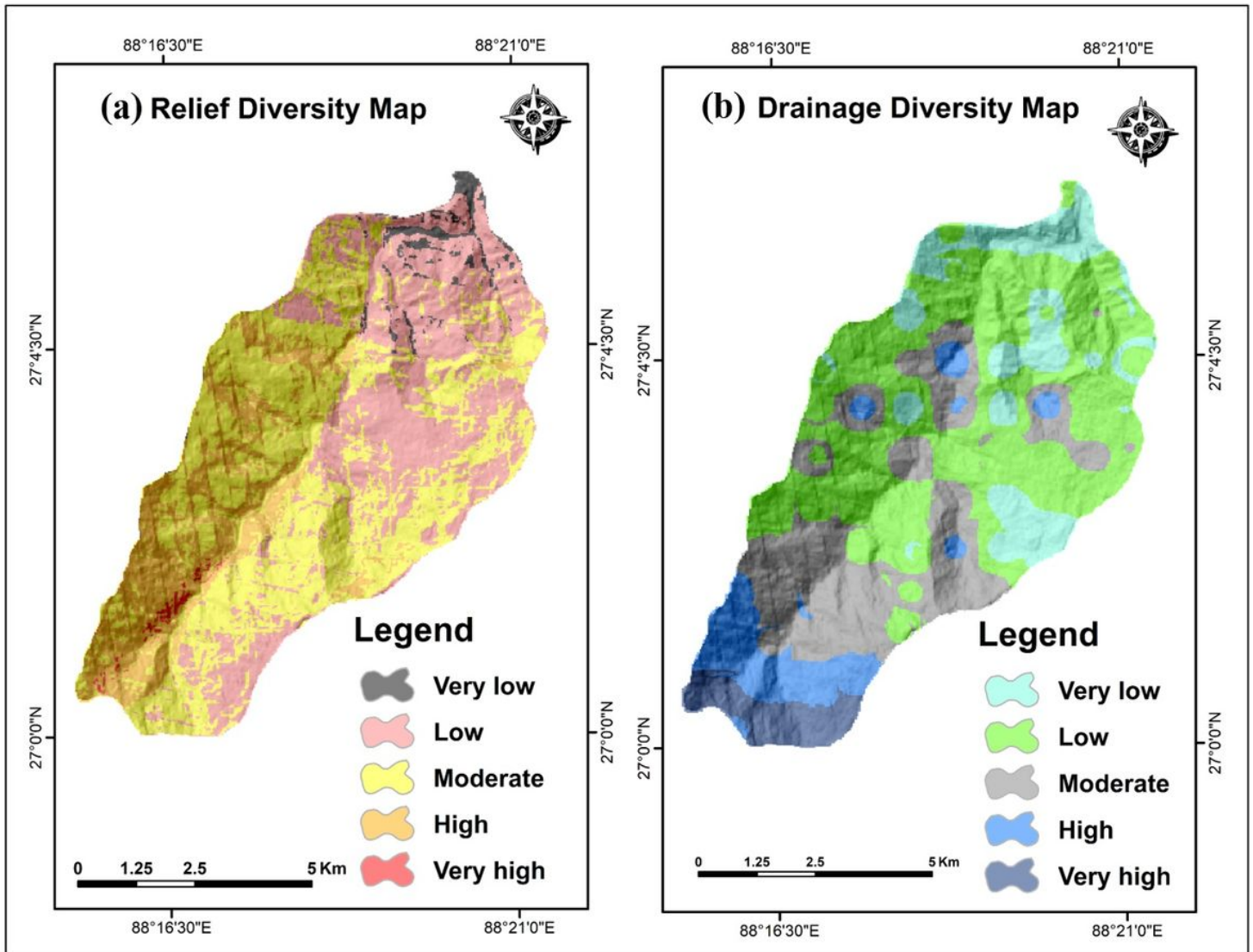


Figure 5

(a) Relief diversity and (b) Drainage diversity maps of the Ragnu Khola River Basin in the Darjeeling Himalaya

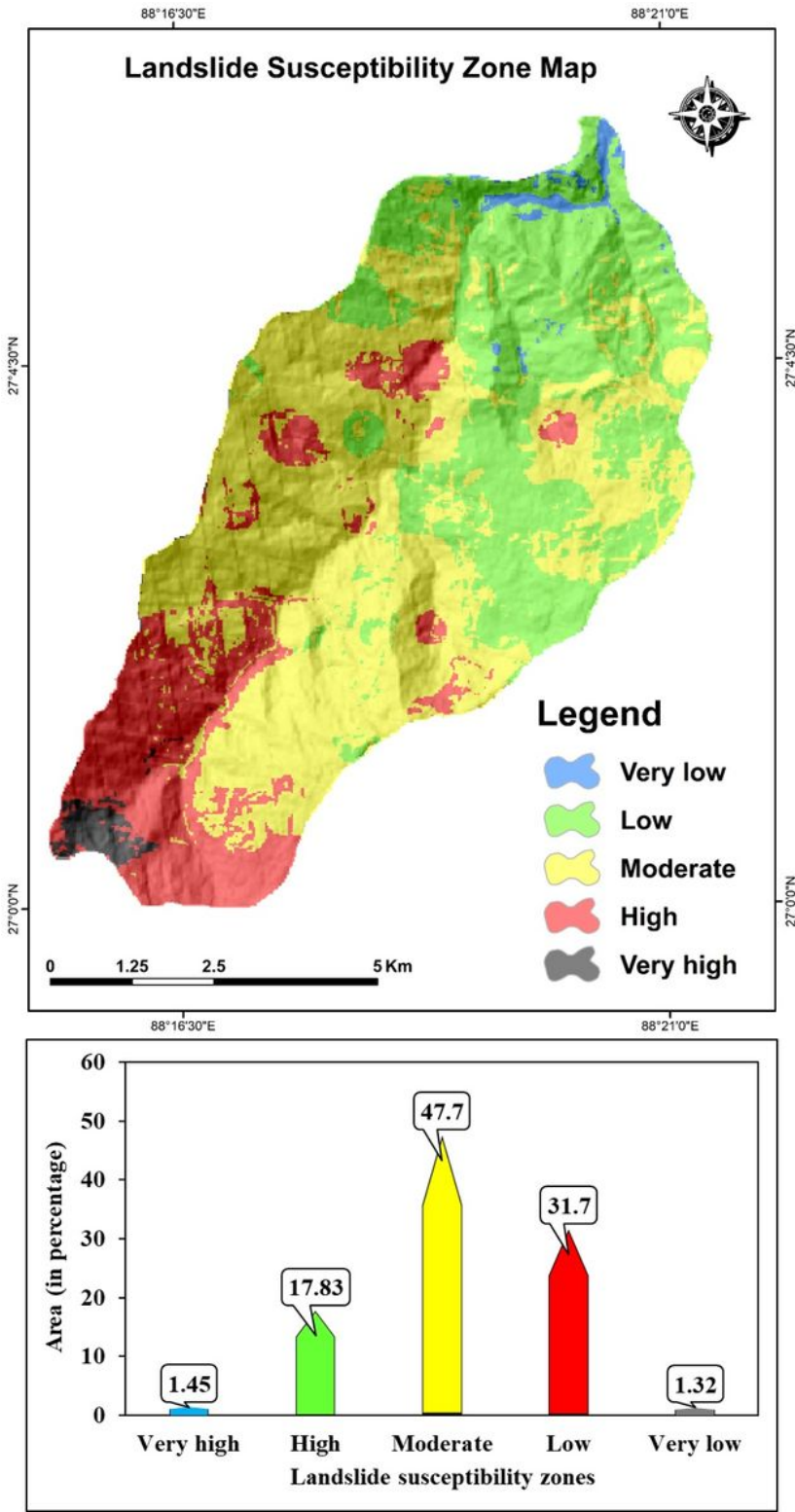


Figure 6

Landslide susceptibility zones in the Ragnu Khola River Basin of Darjeeling Himalaya

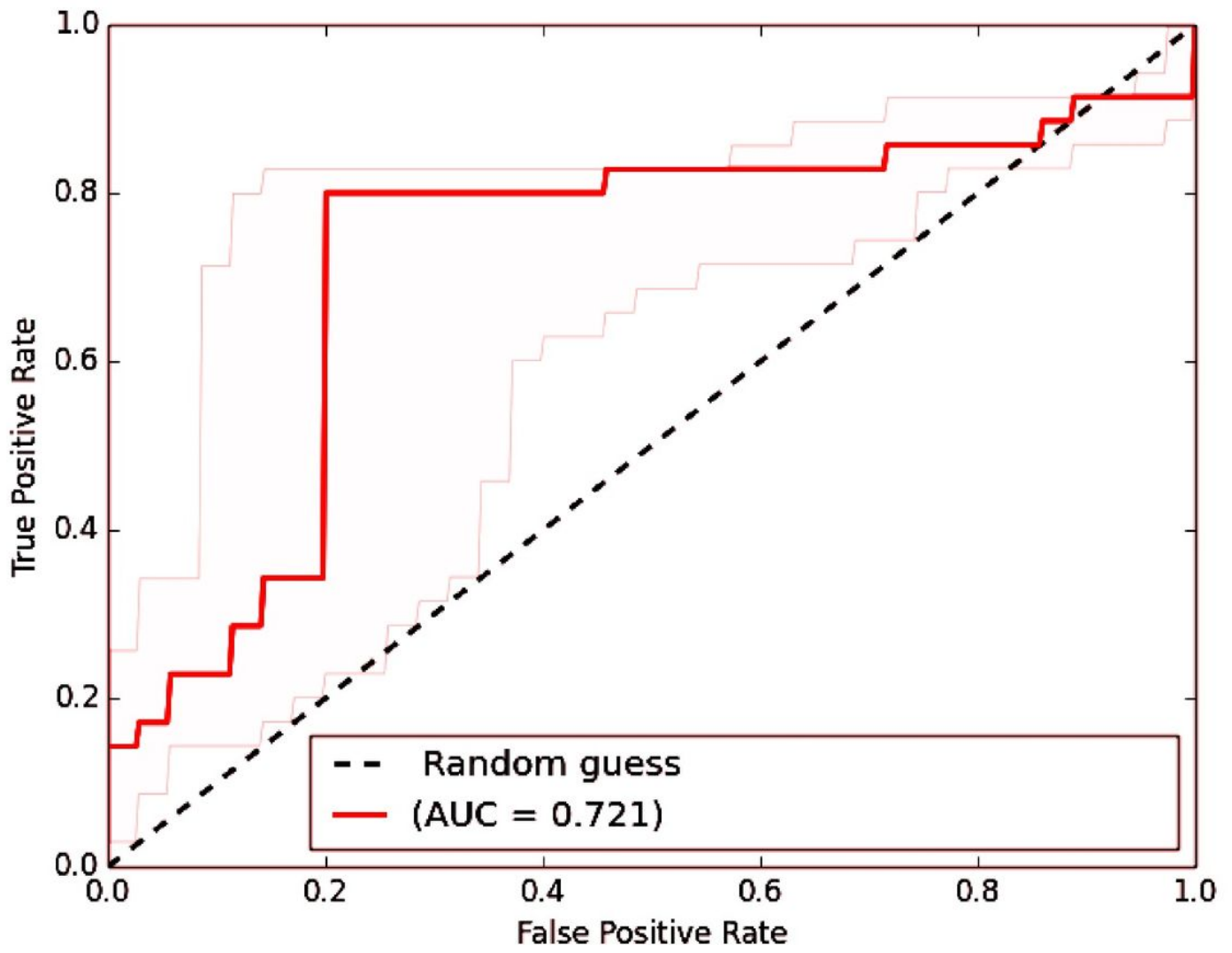


Figure 7

ROC curve for validation of the landslide susceptibility zones



○ **Landslide prone areas**

Figure 8

Landslide prone areas of the Rangu Khola River Basin in the Darjeeling Himalaya (Location: (a) $27^{\circ} 02' 00''\text{N}$, $88^{\circ} 16' 26''\text{E}$, (b) $27^{\circ} 00' 16''\text{N}$, $88^{\circ} 16' 39''\text{E}$, and (c) $27^{\circ} 01' 23''\text{N}$, $88^{\circ} 16' 04''\text{E}$; $27^{\circ} 01' 10''\text{N}$, $88^{\circ} 15' 58''\text{E}$; $27^{\circ} 01' 16''\text{N}$, $88^{\circ} 16' 17''\text{E}$).